

Natural Inflation: status after WMAP 3-year data

Christopher Savage,^{1,*} Katherine Freese,^{1,†} and William H. Kinney^{2,‡}

¹ Michigan Center for Theoretical Physics, Department of Physics, University of Michigan, Ann Arbor, MI 48109

² Department of Physics, University at Buffalo, SUNY, Buffalo, NY 14260

(Dated: February 8, 2020)

The model of Natural Inflation is examined in light of recent 3-year data from the Wilkinson Microwave Anisotropy Probe and shown to provide a good fit. The inflaton potential is naturally flat due to shift symmetries, and in the simplest version takes the form $V(\phi) = \Lambda^4[1 \pm \cos(N\phi/f)]$. The model agrees with WMAP3 measurements as long as $f > 0.7m_{\text{Pl}}$ (where $m_{\text{Pl}} = 1.22 \times 10^{19}$ GeV) and $\Lambda \sim m_{\text{GUT}}$. The running of the scalar spectral index is shown to be small – an order of magnitude below the sensitivity of WMAP3. The location of the field in the potential when perturbations on observable scales are produced is examined; for $f > 5m_{\text{Pl}}$, the relevant part of the potential is indistinguishable from a quadratic, yet has the advantage that the required flatness is well-motivated. Depending on the value of f , the model falls into the large field ($f \geq 1.5m_{\text{Pl}}$) or small field ($f < 1.5m_{\text{Pl}}$) classification scheme that has been applied to inflation models. Natural inflation provides a good fit to WMAP3 data.

I. INTRODUCTION

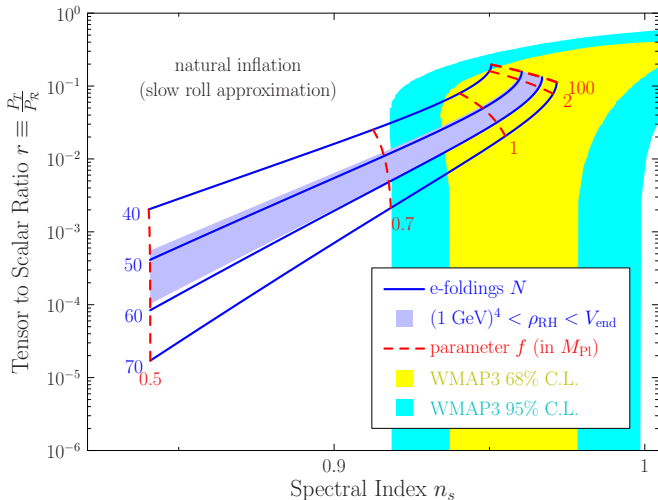


FIG. 1: Natural inflation predictions and WMAP3 constraints in the r - n_s plane. (Solid/blue) lines running from approximately the lower left to upper right are predictions for constant N and varying f , where N is the number of e-foldings prior to the end of inflation at which current modes of scale $k = 0.002 \text{ Mpc}^{-1}$ were generated and f is the width of the potential. The remaining (dashed/red) lines are for constant f and varying N . The (light blue) band corresponds to the values of N for standard post-inflation cosmology with $(1 \text{ GeV})^4 < \rho_{\text{RH}} < V_{\text{end}}$. Filled (nearly vertical) regions are the parameter spaces allowed by WMAP3 at 68% and 95% C.L.’s (error contours taken from Ref. [3]). Natural inflation is consistent with the WMAP3 data for $f \gtrsim 0.7m_{\text{Pl}}$ and essentially all likely values of N .

Inflation was proposed [1] to solve several cosmological puzzles: an early period of accelerated expansion explains the homogeneity, isotropy, and flatness of the universe, as well as the lack of relic monopoles. While inflation results in an approximately homogeneous universe, inflation models also predict small inhomogeneities. Observations of inhomogeneities via the cosmic microwave background (CMB) anisotropies and structure formation are now providing tests of inflation models.

The release of three years of data from the Wilkinson Microwave Anisotropy Probe (WMAP3) [2] satellite have generated a great deal of excitement. First, generic predictions of inflation match the observations: the universe has a critical density ($\Omega = 1$), the density perturbation spectrum is nearly scale invariant, and superhorizon fluctuations are evident. Second, current data is beginning to differentiate between inflationary models and already rules some of them out. For example, quartic potentials and generic hybrid models do not provide a good match to the data [2, 3, 4]. It is the purpose of this paper to illustrate that the model known as Natural Inflation is an excellent match to current data.

Inflation models predict two types of perturbations, scalar and tensor, which result in density and gravitational wave fluctuations, respectively. Each is typically characterized by a fluctuation amplitude ($P_{\mathcal{R}}^{1/2}$ for scalar and $P_T^{1/2}$ for tensor, with the latter usually given in terms of the ratio $r \equiv P_T / P_{\mathcal{R}}$) and a spectral index (n_s for scalar and n_T for tensor) describing the mild scale dependence of the fluctuation amplitude. The amplitude $P_{\mathcal{R}}^{1/2}$ is normalized by the height of the inflationary potential. The inflationary consistency condition $r = -8n_T$ further reduces the number of free parameters to two,

*cmsavage@umich.edu; Also at William I. Fine Theoretical Physics Institute, School of Physics & Astronomy, University of Minnesota, Minneapolis, MN 55455

†ktfreese@umich.edu

‡whkinney@buffalo.edu

leaving experimental limits on n_s and r as the primary means of distinguishing among inflation models. Hence, predictions of models are presented as plots in the r - n_s plane.

Most inflation models suffer from a potential drawback: to match various observational constraints, notably CMB anisotropy measurements as well as the requirement of sufficient inflation, the height of the inflaton potential must be of a much smaller scale than that of the width, by many orders of magnitude (*i.e.*, the potential must be very flat). This requirement of two very different mass scales is what is known as the “fine-tuning” problem in inflation, since very precise couplings are required in the theory to prevent radiative corrections from bringing the two mass scales back to the same level. The natural inflation model (NI) uses shift symmetries to generate a flat potential, protected from radiative corrections, in a natural way [5]. In this regard, NI is one of the best motivated inflation models.

One of the major results of the paper is shown in Figure 1. The predictions of NI are plotted in the r - n_s plane for various parameters: the width f of the potential and number of e-foldings N before the end of inflation at which present day fluctuation modes of scale $k = 0.002 \text{ Mpc}^{-1}$ were produced. N depends upon the post-inflationary universe and is ~ 50 - 60 . Also shown in the figure are the observational constraints from WMAP’s recent 3-year data, which provides some of the tightest constraints on inflationary models to date [2]. The primary result is that NI, for $f \gtrsim 0.7 m_{\text{Pl}}$, is consistent with current observational constraints.

In this paper we take $m_{\text{Pl}} = 1.22 \times 10^{19} \text{ GeV}$. Our result extends upon a previous analysis of NI [6] that was based upon WMAP’s first year data [7].

This paper emphasizes two further results as well. First, we investigate the running of the spectral index in natural inflation, *i.e.* the dependence of n_s on scale, and find that it is small: two orders of magnitude smaller than the sensitivity of WMAP3 and below the sensitivity of any planned experiment. Second, we find how far down the potential the field is at the time structure is produced, and find that for $f > 5 m_{\text{Pl}}$ the relevant part of the potential is indistinguishable from a quadratic potential. (Still, the naturalness motivation for NI renders it a superior model to a quadratic potential as the latter typically lacks an explanation for its flatness).

We will begin by discussing the model of natural inflation in Section II: the motivation, the potential, the evolution of the inflaton field, and relating pre- and post-inflation scales. In Section III, we will examine the scalar and tensor perturbations predicted by NI and compare them with the WMAP 3-year data. In Section IV, we will address the running of the spectral index. In Section V, we will examine the location on the potential at which the observable e-folds of inflation take place and examine where NI falls in the small field/large field/hybrid model categorization scheme. We conclude in Section VI.

II. THE MODEL OF NATURAL INFLATION

Motivation: To satisfy a combination of constraints on inflationary models, in particular, sufficient inflation and microwave background anisotropy measurements [2, 7], the potential for the inflaton field must be very flat. For a general class of inflation models involving a single slowly-rolling field, it has been shown that the ratio of the height to the (width)⁴ of the potential must satisfy [8]

$$\chi \equiv \Delta V / (\Delta \phi)^4 \leq \mathcal{O}(10^{-6} - 10^{-8}), \quad (1)$$

where ΔV is the change in the potential $V(\phi)$ and $\Delta \phi$ is the change in the field ϕ during the slowly rolling portion of the inflationary epoch. Thus, the inflaton must be extremely weakly self-coupled, with effective quartic self-coupling constant $\lambda_\phi < \mathcal{O}(\chi)$ (in realistic models, $\lambda_\phi < 10^{-12}$). The small ratio of mass scales required by Eqn. (1) quantifies how flat the inflaton potential must be and is known as the “fine-tuning” problem in inflation.

Three approaches have been taken toward this required flat potential characterized by a small ratio of mass scales. First, some simply say that there are many as yet unexplained hierarchies in physics, and inflation requires another one. The hope is that all these hierarchies will someday be explained. In these cases, the tiny coupling λ_ϕ is simply postulated *ad hoc* at tree level, and then must be fine-tuned to remain small in the presence of radiative corrections. But this merely replaces a cosmological naturalness problem with unnatural particle physics. Second, models have been attempted where the smallness of λ_ϕ is protected by a symmetry, *e.g.*, supersymmetry. In these cases (*e.g.*, [9]), λ_ϕ may arise from a small ratio of mass scales; however, the required mass hierarchy, while stable, is itself unexplained. In addition, existing models have limitations. It would be preferable if such a hierarchy, and thus inflation itself, arose dynamically in particle physics models.

Hence, in 1990 a third approach was proposed, Natural Inflation [5], in which the inflaton potential is flat due to shift symmetries. Nambu-Goldstone bosons (NGB) arise whenever a global symmetry is spontaneously broken. Their potential is exactly flat due to a shift symmetry under $\phi \rightarrow \phi + \text{constant}$. As long as the shift symmetry is exact, the inflaton cannot roll and drive inflation, and hence there must be additional explicit symmetry breaking. Then these particles become pseudo-Nambu Goldstone bosons (PNGBs), with “nearly” flat potentials, exactly as required by inflation. The small ratio of mass scales required by Eqn. (1) can easily be accommodated. For example, in the case of the QCD axion, this ratio is of order 10^{-64} . While inflation clearly requires different mass scales than the axion, the point is that the physics of PNGBs can easily accommodate the required small numbers.

The NI model was first proposed and a simple analysis performed in [5]. Then, in 1993, a second paper followed which provides a much more detailed study [10]. Many types of candidates have subsequently been explored for

natural inflation. For example, WHK and K.T. Mahanthappa considered NI potentials generated by radiative corrections in models with explicitly broken Abelian [11] and non-abelian [12] symmetries, showing that NI models with $f \sim m_{\text{Pl}}$ and $f \ll m_{\text{Pl}}$ can both be generated in self-consistent field theories. Ref. [13] used shift symmetries in Kahler potentials to obtain a flat potential and drive natural chaotic inflation in supergravity. Additionally, [14, 15] examined natural inflation in the context of extra dimensions and [16] used PNGBs from little Higgs models to drive hybrid inflation. Also, [17, 18] use the natural inflation idea of PNGBs in the context of braneworld scenarios to drive inflation. Freese [19] suggested using a PNGB as the rolling field in double field inflation [20] (in which the inflaton is a tunneling field whose nucleation rate is controlled by its coupling to a rolling field). We will focus in this paper on the original version of natural inflation, in which there is a single rolling field.

Potential: The PNGB potential resulting from explicit breaking of a shift symmetry in single field models (in four spacetime dimensions) is generally of the form

$$V(\phi) = \Lambda^4 [1 \pm \cos(N\phi/f)]. \quad (2)$$

We will take the positive sign in Eqn. (2) (this choice has no effect on our results) and take $N = 1$, so the potential, of height $2\Lambda^4$, has a unique minimum at $\phi = \pi f$ (the periodicity of ϕ is $2\pi f$).

For appropriately chosen values of the mass scales, *e.g.* $f \sim m_{\text{Pl}}$ and $\Lambda \sim m_{\text{GUT}} \sim 10^{15}$ GeV, the PNGB field ϕ can drive inflation. This choice of parameters indeed produces the small ratio of scale required by Eqn. (1), with $\chi \sim (\Lambda/f)^4 \sim 10^{-13}$. While $f \sim m_{\text{Pl}}$ seems to be a reasonable scale for the potential width, there is no reason to believe that f cannot be much larger than m_{Pl} . In fact, Kim, Nilles & Peloso [21] as well as the idea of N-inflation [22] showed that an *effective* potential of $f \gg m_{\text{Pl}}$ can be generated from two or more axions, each with sub-Plankian scales. We shall thus include the possibility of $f \gg m_{\text{Pl}}$ in our analysis and show that these parameters can fit the data.

Evolution of the Inflaton Field: The evolution of the inflaton field is described by

$$\ddot{\phi} + 3H\dot{\phi} + \Gamma\dot{\phi} + V'(\phi) = 0, \quad (3)$$

where Γ is the decay width of the inflaton. A sufficient condition for inflation is the slow-roll (SR) condition $\dot{\phi} \ll 3H\dot{\phi}$. The expansion of the scale factor a , with $H = \dot{a}/a$, is determined by the scalar field dominated Friedmann equation,

$$H^2 = \frac{8\pi}{3m_{\text{Pl}}^2} V(\phi). \quad (4)$$

The slow roll (SR) condition implies that two conditions

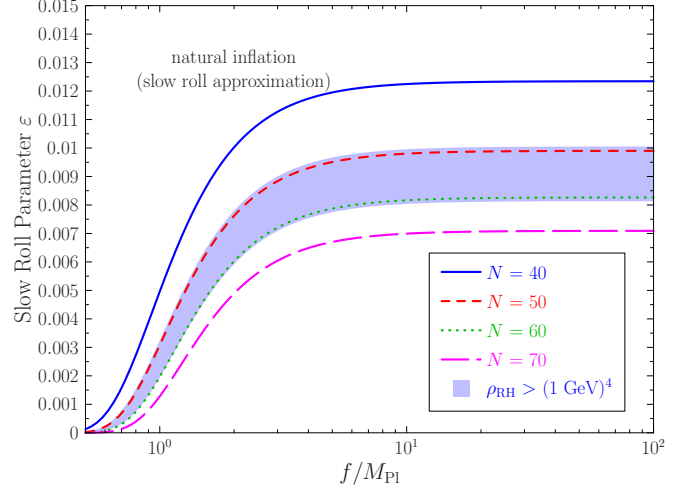


FIG. 2: The slow roll parameter ϵ is shown as a function of the potential width f for various numbers of e-foldings N before the end of inflation. The (light blue) band corresponds to the values of N consistent with the standard post-inflation cosmology, as given by Eqn. (8), for an end of reheating energy density $(1 \text{ GeV})^4 < \rho_{\text{RH}} < V_{\text{end}}$, where the lower bound is a result of nucleosynthesis constraints.

are met:

$$\begin{aligned} \epsilon(\phi) &\approx \frac{m_{\text{Pl}}^2}{16\pi} \left[\frac{V'(\phi)}{V(\phi)} \right]^2 \\ &= \frac{1}{16\pi} \left(\frac{m_{\text{Pl}}}{f} \right)^2 \left[\frac{\sin(\phi/f)}{1 + \cos(\phi/f)} \right]^2 \ll 1 \end{aligned} \quad (5)$$

and

$$\begin{aligned} \eta(\phi) &\approx \frac{m_{\text{Pl}}^2}{8\pi} \left[\frac{V''(\phi)}{V(\phi)} - \frac{1}{2} \left(\frac{V'(\phi)}{V(\phi)} \right)^2 \right] \\ &= -\frac{1}{16\pi} \left(\frac{m_{\text{Pl}}}{f} \right)^2 \ll 1. \end{aligned} \quad (6)$$

Inflation ends when the field ϕ reaches a value ϕ_e such that $\epsilon(\phi_e) < 1$ is violated, or

$$\cos(\phi_e/f) = \frac{1 - 16\pi(f/m_{\text{Pl}})^2}{1 + 16\pi(f/m_{\text{Pl}})^2}. \quad (7)$$

Figure 2 illustrates the value of ϵ during periods where density fluctuations are produced; one can see that indeed $\epsilon \ll 1$.

More accurate results can be attained by numerically solving the equation of motion, Eqn. (3), together with the Friedmann equations. Such calculations have been performed in Ref. [10], where it was shown the SR analysis is accurate to within a few percent for the $f \gtrsim 0.5m_{\text{Pl}}$ parameter space we will be examining. Thus, we are justified in using the SR approximation in our calculations.

Relating Pre- and Post-Inflation Scales: To test inflationary theories, present day observations must be re-

lated to the evolution of the inflaton field during the inflationary epoch. Here we show how a comoving scale k today can be related back to a point during inflation. We need to find the value of N_k , the number of e-foldings before the end of inflation, at which structures on scale k were produced.

Under a standard post-inflation cosmology, once inflation ends, the universe undergoes a period of reheating. Reheating can be instantaneous or last for a prolonged period of matter-dominated expansion. Then reheating ends at $T < T_{RH}$, and the universe enters its usual radiation-dominated and subsequent matter-dominated history. Instantaneous reheating ($\rho_{RH} = \rho_e$) gives the minimum number of e-folds as one looks backwards to the time of perturbation production, while a prolonged period of reheating gives a larger number of e-folds.

The relationship between scale k and the number of e-folds N_k before the end of inflation has been shown to be [23]

$$N_k = 62 - \ln \frac{k}{a_0 H_0} - \ln \frac{10^{16} \text{ GeV}}{V_k^{1/4}} + \ln \frac{V_k^{1/4}}{V_e^{1/4}} - \frac{1}{3} \ln \frac{V_e^{1/4}}{\rho_{RH}^{1/4}} \quad (8)$$

Here, V_k is the potential when k leaves the horizon during inflation, $V_e = V(\phi_e)$ is the potential at the end of inflation, and ρ_{RH} is the energy density at the end of the reheat period. Nucleosynthesis generally requires $\rho_{RH} \gtrsim (1 \text{ GeV})^4$, while necessarily $\rho_{RH} \leq V_e$. Since V_e may be of order $m_{\text{GUT}} \sim 10^{15} \text{ GeV}$ or even larger, there is a broad allowed range of ρ_{RH} ; this uncertainty in ρ_{RH} translates into an uncertainty of 10 e-folds in the value of N_k that corresponds to any particular scale of measurement today.

Henceforth we will use N to refer to the number of e-foldings prior to the end of inflation that correspond to scale $k = 0.002 \text{ Mpc}^{-1}$, the scale at which WMAP presents their results¹. Under the standard cosmology, this scale corresponds to $N \sim 50-60$ (smaller N corresponds to smaller ρ_{RH}), with a slight dependence on f . However, if one were to consider non-standard cosmologies [24], the range of possible N would be broader. Hence we will show results for the more conservative range $40 \leq N \leq 70$, in addition to the more limited standard cosmology range.

III. PERTURBATIONS

As the inflaton rolls down the potential, quantum fluctuations lead to metric perturbations that are rapidly

¹ The current horizon scale corresponds to $k \approx 0.00033 \text{ Mpc}^{-1}$. The difference in these two scales corresponds to only a small difference in e-foldings of $\Delta N \lesssim 2$: while we shall present parameters evaluated at $k = 0.002 \text{ Mpc}^{-1}$, those parameters evaluated at the current horizon scale will have essentially the same values (at the few percent level).

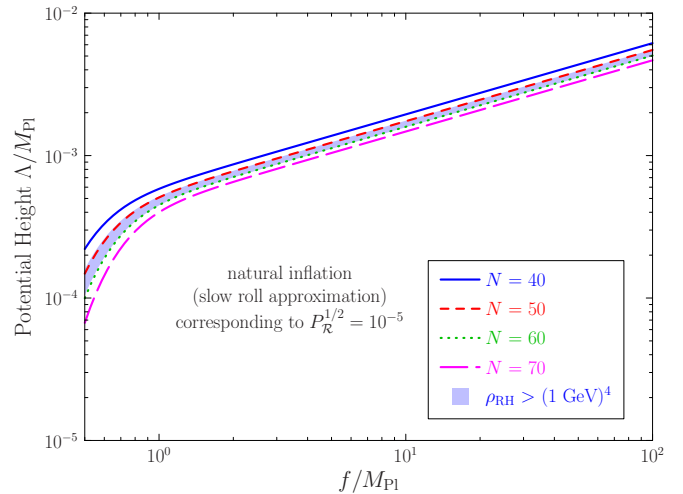


FIG. 3: The potential height scale Λ corresponding to $P_{\mathcal{R}}^{1/2} = 10^{-5}$ is shown as a function of the potential width f for various numbers of e-foldings N before the end of inflation. The (light blue) band corresponds to the values of N consistent with the standard post-inflation cosmology for $\rho_{RH} > (1 \text{ GeV})^4$.

inflated beyond the horizon. These fluctuations are frozen until they re-enter the horizon during the post-inflationary epoch, where they leave their imprint on large scale structure formation and the cosmic microwave background (CMB) anisotropy [25, 26, 27]. In this section, we will examine the scalar (density) and tensor (gravitational wave) perturbations predicted by natural inflation and compare them with the WMAP 3 year (WMAP3) data [2].

A. Scalar (Density) Fluctuations

The perturbation amplitude for the density fluctuations (scalar modes) produced during inflation is given by [28, 29, 30, 31]

$$P_{\mathcal{R}}^{1/2}(k) = \frac{H^2}{2\pi\dot{\phi}_k} \quad (9)$$

Here, $P_{\mathcal{R}}^{1/2}(k) \sim \frac{\delta\rho}{\rho}|_{\text{hor}}$ denotes the perturbation amplitude when a given wavelength re-enters the Hubble radius in the radiation- or matter-dominated era, and the right hand side of Eqn. (9) is to be evaluated when the same comoving wavelength ($2\pi/k$) crosses outside the horizon during inflation.

Normalizing to the COBE [32] or WMAP [2] anisotropy measurements gives $P_{\mathcal{R}}^{1/2} \sim 10^{-5}$. This normalization can be used to approximately fix the height Λ of the potential Eqn. (2). The largest amplitude perturbations on observable scales are those produced $N \sim 60$ e-folds before the end of inflation (corresponding to the horizon

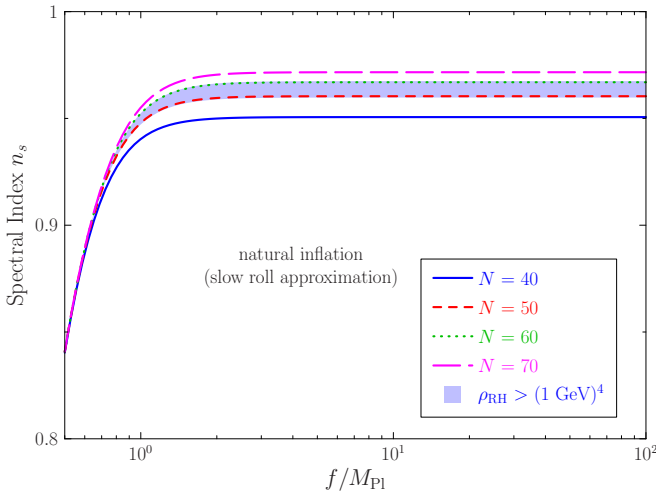


FIG. 4: The spectral index n_s is shown as a function of the potential width f for various numbers of e-foldings N before the end of inflation. The (light blue) band corresponds to the values of N consistent with the standard post-inflation cosmology for $\rho_{RH} > (1 \text{ GeV})^4$.

scale today), when the field value is $\phi = \phi_N$. Under the SR approximation, the amplitude on this scale takes the value

$$P_{\mathcal{R}} \approx \frac{128\pi}{3} \left(\frac{\Lambda}{m_{Pl}} \right)^4 \left(\frac{f}{m_{Pl}} \right)^2 \frac{[1 + \cos(\phi_N/f)]^3}{\sin^2(\phi_N/f)}. \quad (10)$$

The values for Λ corresponding to $P_{\mathcal{R}}^{1/2} = 10^{-5}$ are shown in Figure 3. We see that $\Lambda \sim 10^{15}\text{-}10^{16} \text{ GeV}$ for $f \sim m_{Pl}$, yielding an inflaton mass $m_\phi = \Lambda/f^2 \sim 10^{11}\text{-}10^{13} \text{ GeV}$. Thus, a potential height Λ of the GUT scale and a potential width f of the Planck scale are required in NI in order to produce the fluctuations responsible for large scale structure. For $f \gg m_{Pl}$, the potential height scales as $\Lambda \sim (10^{-3}m_{Pl})\sqrt{f/m_{Pl}}$.

The fluctuation amplitudes are, in general, scale dependent. The spectrum of fluctuations is characterized by the spectral index n_s ,

$$n_s - 1 \equiv \frac{dP_{\mathcal{R}}}{d \ln k} \approx -\frac{1}{8\pi} \left(\frac{m_{Pl}}{f} \right)^2 \frac{3 - \cos(\phi/f)}{1 + \cos(\phi/f)}. \quad (11)$$

The spectral index for natural inflation is shown in Figure 4. For small f , n_s is essentially independent of N , while for $f \gtrsim 2m_{Pl}$, n_s has essentially no f dependence. Analytical estimates can be obtained in these two regimes:

$$n_s \approx \begin{cases} 1 - \frac{m_{Pl}^2}{8\pi f^2}, & \text{for } f \lesssim \frac{3}{4}m_{Pl} \\ 1 - \frac{2}{N}, & \text{for } f \gtrsim 2m_{Pl} \end{cases} \quad (12)$$

The WMAP 3-year data yield $n_s = 0.951^{+0.015}_{-0.019}$ ($n_s = 0.987^{+0.019}_{-0.037}$ when tensor modes are included in the fits)

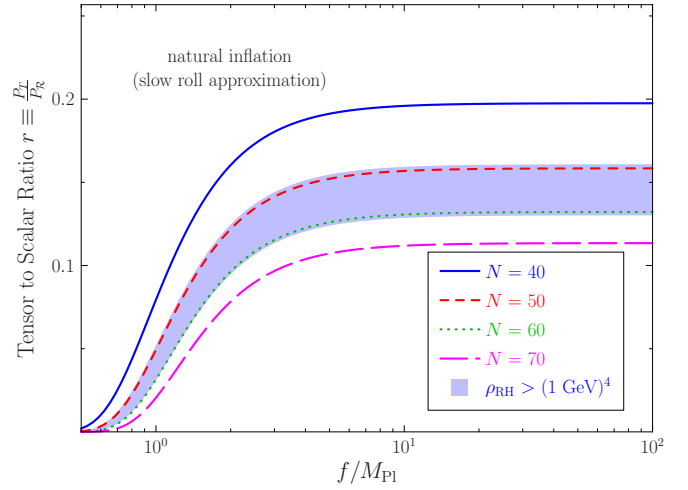


FIG. 5: The tensor to scalar ratio $r \equiv \frac{P_T}{P_{\mathcal{R}}}$ is shown as a function of the potential width f for various numbers of e-foldings N before the end of inflation. The (light blue) band corresponds to the values of N consistent with the standard post-inflation cosmology for $\rho_{RH} > (1 \text{ GeV})^4$.

on the $k = 0.002 \text{ Mpc}^{-1}$ scale². The WMAP3 results lead to the constraint on the width of the natural inflation potential, $f \gtrsim 0.7m_{Pl}$ at 95% C.L.

B. Tensor (Gravitational Wave) Fluctuations

In addition to scalar (density) perturbations, inflation also produces tensor (gravitational wave) perturbations with amplitude

$$P_T^{1/2}(k) = \frac{4H}{\sqrt{\pi}m_{Pl}}. \quad (13)$$

Here, we examine the tensor mode predictions of natural inflation and compare with WMAP data.

Conventionally, the tensor amplitude is given in terms of the tensor/scalar ratio

$$r \equiv \frac{P_T}{P_{\mathcal{R}}} = 16\epsilon, \quad (14)$$

which is shown in Figure 5 for natural inflation. For small f , r rapidly becomes negligible, while $f \rightarrow \frac{8}{N}$ for $f \gg m_{Pl}$. In all cases, $r \lesssim 0.2$, well below the WMAP limit of $r < 0.55$ (95% C.L., no running).

As mentioned in the introduction, in principle, there are four parameters describing scalar and tensor fluctuations: the amplitude and spectra of both components,

² As discussed in Section IV, the running of the spectral index n_s in natural inflation is so small that the value of n_s at the scale of the WMAP3 measurements is virtually identical to its value on the horizon scale.

with the latter characterized by the spectral indices n_s and n_T (we are ignoring any running here). The amplitude of the scalar perturbations is normalized by the height of the potential (the energy density Λ^4). The tensor spectral index n_T is not an independent parameter since it is related to the tensor/scalar ratio r by the inflationary consistency condition $r = -8n_T$. The remaining free parameters are the spectral index n_s of the scalar density fluctuations, and the tensor amplitude (given by r).

Hence, a useful parameter space for plotting the model predictions versus observational constraints is on the r - n_s plane [33, 34]. Natural inflation generically predicts a tensor amplitude well below the detection sensitivity of current measurements such as WMAP. However, the situation will improve markedly in future experiments with greater sensitivity such as QUIET [35] and PLANCK [36], as well as proposed experiments such as CMBPOL [37].

In Figure 1, we show the predictions of natural inflation for various choices of the number of e-folds N and the mass scale f , together with the WMAP3 observational constraints. Parameters corresponding to fixed $N = (40, 50, 60, 70)$ with varying f are shown as (solid/blue) lines from the lower left to upper right. The orthogonal (dashed/red) lines correspond to fixed f with varying N . The (blue) band are the values of N consistent with standard post-inflation cosmology for reheat temperatures above the nucleosynthesis limit of ~ 1 GeV, as discussed previously. The solid regions are the WMAP3 allowed parameters at 68% and 95% C.L.'s. For a given N , a fixed point is reached for $f \gg m_{\text{Pl}}$; that is, r and n_s become essentially independent of f for any $f \gtrsim 10m_{\text{Pl}}$. This is apparent from the $f = 10m_{\text{Pl}}$ and $f = 100m_{\text{Pl}}$ lines in the figure, which are both shown, but are indistinguishable. As seen in the figure, $f \lesssim 0.7m_{\text{Pl}}$ is excluded. However, $f \gtrsim 0.8m_{\text{Pl}}$ falls well into the WMAP3 allowed region and is thus consistent with the WMAP3 data.

IV. RUNNING OF THE SPECTRAL INDEX

In general, n_s is not constant: its variation can be characterized by its running, $\frac{dn_s}{d \ln k}$. In this section, we use numerical solutions to the equation of motion, Eqn. (3), as the slow roll approximation (to the order used throughout this paper) is inaccurate for determining the running. As shown in Figure 6, natural inflation predicts a small, $\mathcal{O}(10^{-3})$, negative spectral index running. This is negligibly small for WMAP sensitivities and this model is essentially indistinguishable from zero running in the WMAP analysis. While WMAP data prefer a non-zero, negative running of $\mathcal{O}(10^{-1})$ when running is included in the analysis, zero running is not excluded at 95% C.L. Small scale CMB experiments such as CBI [38], ACBAR [39], and VSA [40] will provide more stringent tests of the running and hence of specific inflation models. The

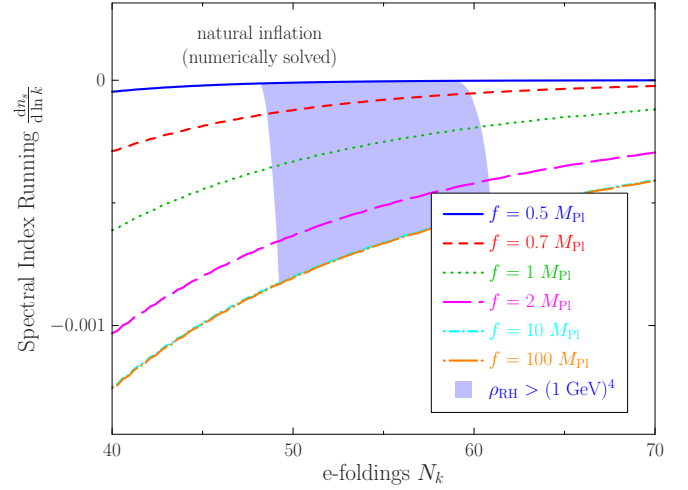


FIG. 6: The spectral index running $\frac{dn_s}{d \ln k}$ is shown as a function of the number of e-foldings N_k before the end of inflation for several values of the potential width f (note that larger N_k corresponds to smaller values of k as in Eqn. (8). The (light blue) filled region corresponds to the values of N consistent with the standard post-inflation cosmology for $\rho_{\text{RH}} > (1 \text{ GeV})^4$.

predicted running for NI is too small to be detected in even these experiments: if these experiments definitively detect a strong running (*i.e.*, excluding a zero/trivial running), natural inflation in the form discussed here would be ruled out.

V. INFLATON POTENTIAL AND INFLATIONARY MODEL SPACE

In this section, we will examine the evolution of the inflaton field ϕ along the potential. We will show that the location on the potential at which the final ~ 60 e-foldings of inflation occurs depends on the width f of the potential. We will also show that natural inflation can fall into either the ‘large field’ or ‘small field’ categorization defined by [33], depending again on the value of f .

The natural inflation potential is shown in Figure 7. For comparison, a quadratic expansion about the minimum at $\phi = \pi f$ is also shown. Inflation occurs when the field slowly rolls down the potential and ends at the point where the field begins to move rapidly (technically, when $\epsilon \geq 1$). In the right panel of the figure, we show the location along the potential where inflation ends ($N_k = 0$) for various values of the potential width f . In the left panel, the location along the potential is shown at $N_k = 60$ e-foldings prior to the end of inflation, the approximate time when fluctuations were produced that correspond to the current horizon. This is not necessarily where inflation began: the field may have started at any point further up the potential and produced more than 60 e-foldings of expansion. The rolling of the field above these

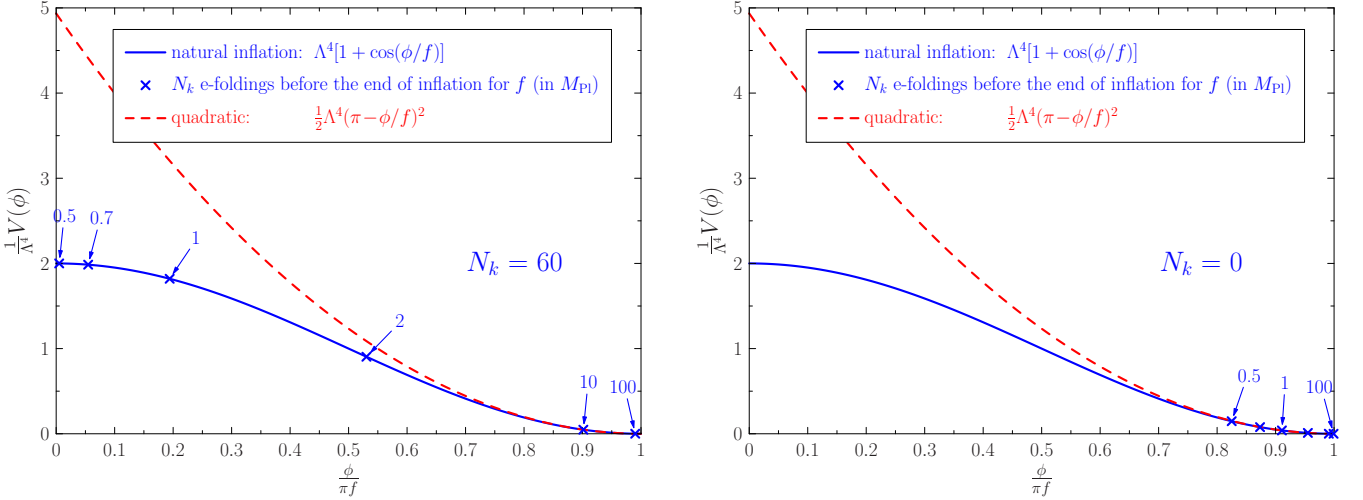


FIG. 7: The natural inflation potential is shown, along with a quadratic expansion around the potential minimum. Also shown are the positions on the potential at 60 e-foldings prior to the end of inflation (left panel) and at the end of inflation (right panel) for potential widths $f = (0.5, 0.7, 1, 2, 10, 100)m_{\text{Pl}}$. For $f \gtrsim 3m_{\text{Pl}}$, the relevant portion of the potential is essentially quadratic during the last 60 e-foldings of inflation.

points, however, would have produced modes which are still on super-horizon scales today and hence are unobservable. In the following discussion, we will be referring only to the *observable* ($N_k \lesssim 60$) portion of the inflaton evolution. For all $f \gtrsim 0.5m_{\text{Pl}}$, inflation ends somewhere near the bottom of the potential, with inflation for larger f ending farther down the potential than for smaller f . We can see, however, that the start of the observable portion of rolling is spread widely over the potential. For $f \lesssim 1m_{\text{Pl}}$, current horizon modes were produced while the field was near the top of the potential. Conversely, for $f \gtrsim 3m_{\text{Pl}}$, those modes were produced near the bottom of the potential. For $f \geq 5m_{\text{Pl}}$, the observationally relevant portion of the potential is essentially a ϕ^2 potential; note, however, that in natural inflation this effectively power law potential is produced via a natural mechanism.

Due to the variety of inflation models, there have been attempts to classify models into a few groups. Dodelson, Kinney & Kolb [33] have proposed a scheme with three categories: small field, large field, and hybrid inflation models, which are easily distinguishable in the SR approximation by the SR parameters ϵ and η . Small field models are characterized by $V''(\phi) < 0$ and $\eta < -\epsilon$, large field models by $V''(\phi) > 0$ and $-\epsilon < \eta \leq \epsilon$, and hybrid models by $V''(\phi) > 0$ and $\eta > \epsilon > 0$. To first order in slow roll, $n_s = 1 - 4\epsilon - 2\eta$ and $r = 16\epsilon$, so the categories have distinct regions in the r - n_s plane, as shown in Figure 8. Also shown in the figure are the predictions for natural inflation; parameters are labeled as in Figure 1 (which showed the same predictions, albeit with a logarithmic rather than linear scale). From Figure 8, it can be seen that natural inflation does not fall into a single category, but may be either small field or large field, depending on the potential width f . This should not be surprising from the preceding discussion of

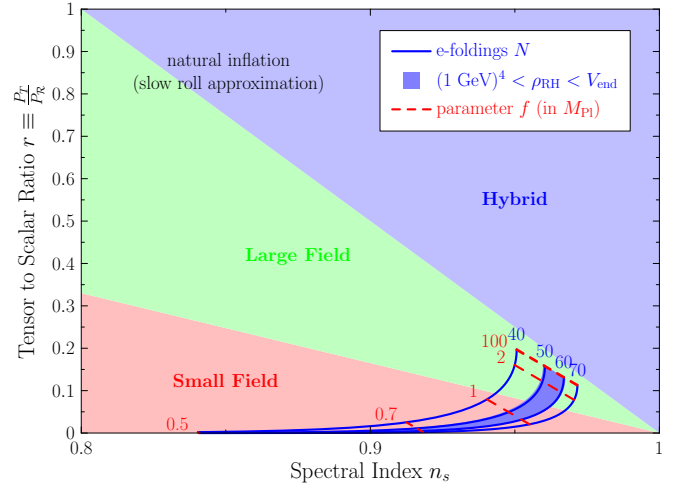


FIG. 8: Natural inflation predictions in the r - n_s plane (parameters and regions labeled as in Figure 1), as well as the regions classifying small field, large field, and hybrid inflation models. Natural inflation falls into different classes depending on the potential width f : for $f \lesssim 1.5m_{\text{Pl}}$, natural inflation can be classified as a small field model, while for $f \gtrsim 1.5m_{\text{Pl}}$, natural inflation can be classified as a large field model.

the potential. For $f \lesssim 1.5m_{\text{Pl}}$, ϕ is on the upper part of the potential, where $V''(\phi) < 0$, at $N_k = 60$ and, thus, falls into the small field regime. For $f \gtrsim 1.5m_{\text{Pl}}$, ϕ is lower down the potential, where $V''(\phi) > 0$, at $N_k = 60$ and falls into the large field regime along with power law ($V(\phi) \sim \phi^p$ for $p > 1$) models [41]. The WMAP3 constraints shown in Figure 1 and discussed in Section III, requiring $f \gtrsim 0.7m_{\text{Pl}}$, still allow natural inflation to fall into either of the small or large field categories.

VI. CONCLUSION

Remarkable advances in cosmology have taken place in the past decade thanks to Cosmic Microwave Background experiments. The release of the 3 year data set by the Wilkinson Microwave Anisotropy Probe is leading to exciting times for inflationary cosmology. Not only are generic predictions of inflation confirmed (though there are still outstanding theoretical issues), but indeed individual inflation models are beginning to be tested.

Currently the natural inflation model, which is extremely well-motivated on theoretical grounds of naturalness, is a good fit to existing data. In this paper, we showed that for potential width $f > 0.7m_{\text{Pl}}$ and height $\Lambda \sim m_{\text{GUT}}$ the model is in good agreement with WMAP3 data. Natural inflation predicts very little running, an order of magnitude lower than the sensitivity of WMAP. The location of the field in the potential while perturbations on observable scales are produced was shown to depend on the width f . Even for values $f > 5m_{\text{Pl}}$ where the relevant parts of the potential are indistinguishable from quadratic, natural inflation provides a framework free of fine-tuning for the required potential.

There has been some confusion in the literature as to whether natural inflation should be characterized as a ‘small-field’ or ‘large-field’ model. In Figure 8 we demonstrated that either categorization is possible, depending on the value of f , and that both are in agreement with data.

Natural inflation makes definite predictions for tensor modes, as shown in Figure 1. Polarization measurements in the next decade have the capability of testing these predictions and of nailing down the right type of inflationary potentials.

Acknowledgments

CS and KF acknowledge the support of the DOE and the Michigan Center for Theoretical Physics via the University of Michigan. CS also acknowledges the support of the William I. Fine Theoretical Physics Institute at the University of Minnesota. WHK is supported in part by the National Science Foundation under grant NSF-PHY-0456777. KF thanks R. Easter and L. Verde for useful discussions.

[1] A. H. Guth, Phys. Rev. D **23**, 347 (1981).
[2] D. N. Spergel *et al.*, arXiv:astro-ph/0603449.
[3] W. H. Kinney, E. W. Kolb, A. Melchiorri and A. Riotto, Phys. Rev. D **74**, 023502 (2006) [arXiv:astro-ph/0605338].
[4] L. Alabidi and D. H. Lyth, arXiv:astro-ph/0603539.
[5] K. Freese, J. A. Frieman and A. V. Olinto, Phys. Rev. Lett. **65**, 3233 (1990).
[6] K. Freese and W. H. Kinney, Phys. Rev. D **70**, 083512 (2004) [arXiv:hep-ph/0404012].
[7] D. N. Spergel *et al.* [WMAP Collaboration], Astrophys. J. Suppl. **148**, 175 (2003) [arXiv:astro-ph/0302209].
[8] F. C. Adams, K. Freese and A. H. Guth, Phys. Rev. D **43**, 965 (1991).
[9] R. Holman, P. Ramond and G. G. Ross, Phys. Lett. B **137**, 343 (1984).
[10] F. C. Adams, J. R. Bond, K. Freese, J. A. Frieman and A. V. Olinto, Phys. Rev. D **47**, 426 (1993) [arXiv:hep-ph/9207245].
[11] W. H. Kinney and K. T. Mahanthappa, Phys. Rev. D **52**, 5529 (1995) [arXiv:hep-ph/9503331].
[12] W. H. Kinney and K. T. Mahanthappa, Phys. Rev. D **53**, 5455 (1996) [arXiv:hep-ph/9512241].
[13] M. Kawasaki, M. Yamaguchi and T. Yanagida, Phys. Rev. Lett. **85**, 3572 (2000) [arXiv:hep-ph/0004243].
[14] N. Arkani-Hamed, H. C. Cheng, P. Creminelli and L. Randall, Phys. Rev. Lett. **90**, 221302 (2003) [arXiv:hep-th/0301218].
[15] N. Arkani-Hamed, H. C. Cheng, P. Creminelli and L. Randall, JCAP **0307**, 003 (2003) [arXiv:hep-th/0302034].
[16] D. E. Kaplan and N. J. Weiner, JCAP **0402**, 005 (2004) [arXiv:hep-ph/0302014].
[17] H. Firouzjahi and S. H. H. Tye, Phys. Lett. B **584**, 147 (2004) [arXiv:hep-th/0312020].
[18] J. P. Hsu and R. Kallosh, JHEP **0404**, 042 (2004) [arXiv:hep-th/0402047].
[19] K. Freese, Phys. Rev. D **50**, 7731 (1994) [arXiv:astro-ph/9405045].
[20] F. C. Adams and K. Freese, Phys. Rev. D **43**, 353 (1991) [arXiv:hep-ph/0504135].
[21] J. E. Kim, H. P. Nilles and M. Peloso, JCAP **0501**, 005 (2005) [arXiv:hep-ph/0409138].
[22] S. Dimopoulos, S. Kachru, J. McGreevy and J. G. Wacker, arXiv:hep-th/0507205.
[23] J. E. Lidsey, A. R. Liddle, E. W. Kolb, E. J. Copeland, T. Barreiro and M. Abney, Rev. Mod. Phys. **69**, 373 (1997) [arXiv:astro-ph/9508078].
[24] A. R. Liddle and S. M. Leach, Phys. Rev. D **68**, 103503 (2003) [arXiv:astro-ph/0305263].
[25] A. H. Guth and S. Y. Pi, Phys. Rev. Lett. **49**, 1110 (1982).
[26] S. W. Hawking, Phys. Lett. B **115**, 295 (1982).
[27] A. A. Starobinsky, Phys. Lett. B **117**, 175 (1982).
[28] V. F. Mukhanov, JETP Lett. **41**, 493 (1985) [Pisma Zh. Eksp. Teor. Fiz. **41**, 402 (1985)].
[29] V. F. Mukhanov, Sov. Phys. JETP **67**, 1297 (1988) [Zh. Eksp. Teor. Fiz. **94N7**, 1 (1988)].
[30] V. F. Mukhanov, H. A. Feldman and R. H. Brandenberger, Phys. Rept. **215**, 203 (1992).
[31] E. D. Stewart and D. H. Lyth, Phys. Lett. B **302**, 171 (1993) [arXiv:gr-qc/9302019].
[32] G. F. Smoot *et al.*, Astrophys. J. **396**, L1 (1992).
[33] S. Dodelson, W. H. Kinney and E. W. Kolb, Phys. Rev. D **56**, 3207 (1997) [arXiv:astro-ph/9702166].
[34] W. H. Kinney, Phys. Rev. D **58**, 123506 (1998) [arXiv:astro-ph/9806259].
[35] See *e.g.* B. Winstein, 2nd Irvine Cosmology Conference

(2006).

- [36] [Planck Collaboration], arXiv:astro-ph/0604069.
- [37] J. Bock *et al.*, arXiv:astro-ph/0604101.
- [38] B. S. Mason *et al.*, *Astrophys. J.* **591**, 540 (2003) [arXiv:astro-ph/0205384].
- [39] C. I. Kuo *et al.* [ACBAR collaboration], *Astrophys. J.* **600**, 32 (2004) [arXiv:astro-ph/0212289].
- [40] C. Dickinson *et al.*, *Mon. Not. Roy. Astron. Soc.* **353**, 732 (2004) [arXiv:astro-ph/0402498].
- [41] L. Alabidi and D. H. Lyth, *JCAP* **0605**, 016 (2006) [arXiv:astro-ph/0510441].